

and (A23) depend upon which fine structure component is being considered because the g factor is given by

$$g_F = g_J \left(\frac{F(F+1) + J(J+1) - I(I+1)}{2F(F+1)} \right). \quad (\text{A24})$$

[†]Work partially supported by a grant from the National Aeronautics and Space Administration.

¹J. B. H. Stedeford and J. B. Hasted, Proc. Roy. Soc. (London) **A227**, 474 (1954).

²G. H. Dunn, R. Geballe, and D. Pretzer, Phys. Rev. **128**, 2200 (1962); G. H. Dunn, R. Geballe, and D. Pretzer, in *Proceedings of the Second International Conference on the Physics of Electronic and Atomic Collisions*, Boulder, Colorado, 1961 (Benjamin, New York, 1961), p. 26.

³V. A. Gusev, G. N. Polyakova, V. F. Erko, Ya. M. Fogel, and A. V. Zats, in *Abstracts of the Sixth International Conference on the Physics of Electronic and Atomic Collisions* (MIT Press, Cambridge, Mass., 1969), p. 809.

⁴R. D. Nathan and R. C. Isler, Phys. Rev. Letters **26**, 1091 (1971).

⁵R. J. Van Brunt and R. N. Zare, J. Chem. Phys. **48**, 4304 (1968).

⁶W. L. Wiese, M. W. Smith, and B. M. Glennon, *Atomic Transition Probabilities*, Natl. Bur. Std. Ref. Data Ser. 4 (U.S. GPO, Washington, D. C., 1966), Vol. 1.

⁷R. A. Young, R. F. Stebbings, J. W. McGowan, Phys. Rev. **171**, 85 (1968).

⁸F. T. Smith, H. H. Fleischmann, and R. A. Young, Phys. Rev. A **2**, 379 (1970).

⁹W. R. Ott, W. E. Kauppila, and W. L. Fite, Phys. Rev. A **1**, 1089 (1970); D. A. Vroom and F. J. DeHeer,

J. Chem. Phys. **50**, 580 (1969).

¹⁰W. E. Kauppila, P. J. O. Teubner, W. L. Fite, and R. J. Girnius, Phys. Rev. A **2**, 1759 (1970).

¹¹D. R. Bates, K. Ledsham, and A. L. Stewart, Phil. Trans. Roy. Soc. London **A246**, 215 (1954).

¹²M. Kotani, K. Ohno, and K. Kayama, *Handbuch der Physik* (Springer, Berlin, 1961), Vol. XXXVII/II, p. 56; P. M. Morse and E. C. G. Stueckelberg, Phys. Rev. **33**, 932 (1929).

¹³R. H. McKnight, Bull. Am. Phys. Soc. **16**, 1355 (1971).

¹⁴The excitation matrix is taken to be diagonal in F because we are concerned here only with zero field level crossings. The observation of high-field crossings between sublevels of different total angular momentum states may prove to be useful in determining populations of substates or to be necessary for precise fits to depolarization curves, but the accuracy of the current measurements do not warrant consideration of these factors in the present development.

¹⁵A. R. Edmonds, *Angular Momentum in Quantum Mechanics*, 2nd ed. (Princeton U. P., Princeton, New Jersey, 1960).

¹⁶The form of Eq. (7) assumes that the energies of the magnetic sublevels are linear functions of the external field strength; i. e., that F , or in the limit of complete nuclear decoupling J , is a good quantum number. In the intermediate field case, the energies must be computed by diagonalizing the matrix for the Zeeman effect.

Photoionization Accompanied by Excitation of Fe I[†]

Hugh P. Kelly

Department of Physics, University of Virginia, Charlottesville, Virginia 22901

(Received 7 April 1972)

The author has calculated contributions to the total photoionization cross section of Fe I in which the remaining Fe II ion is left in a low-lying excited state. The excited states considered are $(3d)^7 4P$, $4F$ and $(3d)^6 5D 4p 6D$, $6F$, $6P$, $4F$, $4D$, and $4P$. We used the velocity form for the dipole-matrix elements and calculated the cross sections by means of many-body perturbation theory. Our results are compared with the cross section for photoionization of Fe I without excitation which we calculated recently. Near threshold the contributions to the total photoionization cross section involving excited $(3d)^7$ and $(3d)^6 5D 4p$ excited states of Fe I are approximately 20% of the cross section without excitation.

I. INTRODUCTION

Atomic photoionization cross sections are very useful in probing the details of atomic structure and they are also of importance in other areas of physics, particularly astrophysics.¹ It is important for the atomic theorist to be able to make accurate *a priori* calculations of atomic photo-cross-sections. When accurate experimental cross sections

exist, the calculations serve as a test of atomic theories and methods of calculation. Once an accurate method of calculation has been established, it can be used to predict cross sections for those cases where experimental results do not yet exist.¹

Recently we have calculated the photoionization cross section of the neutral iron atom from threshold to 10 keV.² The calculation was motivated both by its usefulness for astrophysics³ and also as an

example of the use of many-body perturbation theory^{4,5} in atomic physics.⁶ Although correlation effects in the initial and final states were included to lowest order in perturbation theory, there remain new physical effects which are described by higher-order terms in the perturbation expansion and may contribute significantly to the cross section. Among the most interesting are those in which the incident photon causes the ejection of an electron with the simultaneous excitation of the remaining ion. As yet, we do not have information about such processes for many atoms. However, there have been experimental studies^{7,8} for He in which there is excitation to the $n=2$ level of He^+ . There have also been calculations⁹⁻¹¹ of the cross section with excitation to the $n=2$ level of He^+ . It is found^{7,8} that near threshold for photoionization along with $n=2$ excitation of He^+ there is a contribution from this process of approximately 9% to the total cross section. Photoionization accompanied by excitation has also been studied recently for Ne by Wulleumier and Krause¹² who find that multiple processes (including double photoionization) constitute approximately 20% of the total cross section over a wide range of energies.

For more complicated ions such as FeI which have many relatively low-lying excited states, one might expect a larger contribution to the total cross section from excitation processes. We note that the total of all such contributions involves a sum over the infinite number of bound excited states and also includes the contribution from double (and higher) photoionization.

II. THEORY AND METHODS

In using many-body perturbation theory to calculate the photoionization cross section $\sigma(\omega)$, it is convenient to use the relation²

$$\sigma(\omega) = (4\pi\omega/c) \text{Im}\alpha(\omega), \quad (1)$$

where $\alpha(\omega)$ is the frequency-dependent polarizability, ω is the photon energy in atomic units, and c is the speed of light (137.036 in a.u.). Atomic units are used throughout this paper unless specified otherwise. The frequency-dependent polarizability¹³ $\alpha(\omega)$ and its perturbation expansion in terms of diagrams have been discussed previously.^{2,14,15} The exact expression for $\alpha(\omega)$ is given by¹³

$$\alpha(\omega) = -\sum_k' |\langle k|z|p\rangle|^2 \left(\frac{1}{\epsilon_p - \epsilon_k - \omega} + \frac{1}{\epsilon_p - \epsilon_k + \omega} \right), \quad (2)$$

where the initial state $|p\rangle$ and intermediate states $|k\rangle$ represent exact eigenstates of the Hamiltonian

$$H = \sum_{i=1}^N \left(-\frac{\nabla_i^2}{2} - \frac{Z}{r_i} \right) + \sum_{i<j} r_{ij}^{-1}, \quad (3)$$

with $H|p\rangle = \epsilon_p|p\rangle$ and $H|k\rangle = \epsilon_k|k\rangle$. The prime on the summation indicates a sum over all intermediate states different from $|p\rangle$. The operator z represents $\sum_{i=1}^N z_i$. Since $\epsilon_p - \epsilon_k + \omega$ may vanish, we add a small imaginary part $i\eta$ and note that

$$\lim_{\eta \rightarrow 0} (\epsilon_p - \epsilon_k + \omega + i\eta)^{-1} = \mathcal{P}(\epsilon_p - \epsilon_k + \omega)^{-1} - i\pi\delta(\epsilon_p - \epsilon_k + \omega), \quad (4)$$

where \mathcal{P} represents a principal value integration. We replace \sum_k' by $(2/\pi) \int_0^\infty dk$ for continuum states assuming continuum states are normalized according to⁶

$$R_k(r) \sim \frac{\cos[kr + \delta_l + (q/k) \ln 2kr - \frac{1}{2}(l+1)\pi]}{r} \text{ as } r \rightarrow \infty, \quad (5)$$

where $V(r) \rightarrow q/r$. Using Eqs. (2), (4), and (5), one finds²

$$\text{Im}\alpha(\omega) = (2/k) |\langle k|z|p\rangle|^2, \quad (6)$$

where $k = (2\epsilon_p + 2\omega)^{1/2}$.

We note that the matrix elements $\langle k|z|p\rangle$ may also be written in the velocity form according to¹⁶

$$\langle k|z|p\rangle = (-\omega_{kp})^{-1} \left\langle k \left| \frac{d}{dz} \right| p \right\rangle, \quad (7)$$

where $\omega_{kp} = (\epsilon_k - \epsilon_p)$.

In atomic problems we do not in general know the matrix elements for exact states $|k\rangle$ and $|p\rangle$ of the Hamiltonian of Eq. (3), but we may resort to perturbation theory to obtain approximately exact states and matrix elements.⁶ For example, we may use many-body perturbation theory to obtain $\text{Im}\alpha(\omega)$ in a diagrammatic expansion.² The diagrams for $\text{Im}\alpha(\omega)$ may also be decomposed into "open diagrams"² contributing to the exact matrix elements $\langle k|z|p\rangle$. Examples are given in Fig. 2 of Ref. 2 in which there are only single-electron excitations in the final state. In drawing such diagrams, one is also led to consider those diagrams

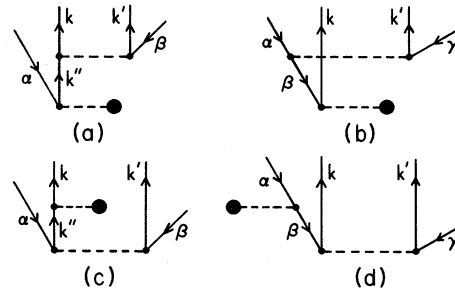


FIG. 1. Lowest-order diagrams contributing to photoionization with excitation. The final many-particle state contains two excited single-particle $|k\rangle$ and $|k'\rangle$, at least one of which is a continuum state.

in which the final state contains two single-particle excitations relative to the initial state. The lowest order diagrams contributing to such double excitations are shown in Fig. 1. In the final many-particle state there are electrons in excited single-particle states $|k\rangle$ and $|k'\rangle$ due to excitations from unexcited states $|\alpha\rangle$ and $|\beta\rangle$ in diagrams (a) and (c) and from unexcited states $|\alpha\rangle$ and $|\gamma\rangle$ in diagrams (b) and (d). In Fig. 1, the heavy dot represents the dipole interaction with either z or d/dz which are related through Eq. (7). The order of interactions is from bottom to top in the diagrams. In diagrams (a) and (b) there is a correlation interaction following the dipole interaction and this represents correlations in the final state. In diagrams (c) and (d) the correlation interaction occurs first and this represents correlation in the initial state. The diagrams in Fig. 1 have been considered previously^{17,18} in connection with the double photoeffect, i. e., where two electrons are ejected into the continuum. In this paper we calculate the diagrams of Fig. 1 for the neutral iron atom when one of the states $|k\rangle$ and $|k'\rangle$ is a continuum state and the other is a low-lying bound excited state. The diagrams are evaluated by the methods of Ref. 6.

III. RESULTS AND CONCLUSIONS

The low-lying states of Fe II which are obtained by the diagrams of Fig. 1 with a $4s-3d$ excitation with a $(3d)^6 5D$ core are $(3d)^7 4F$ and $4P$. The $4s-4p$ excitations couple with the $(3d)^6 5D$ core to give excited Fe II states $(3d)^6 5D(4p) 6D, 6F, 6P, 4F, 4D,$ and $4P$. The energies of these levels are given by Moore.¹⁹ For the $4s-3d$ excitations, the ejected continuum electron may have either $l=1$ or $l=3$. For the $4s-4p$ excitations, continuum states with $l=0$ and $l=2$ are allowed. In order to obtain the contributions of the diagrams of Fig. 1 to these multiplets of Fe II, we project the determinants

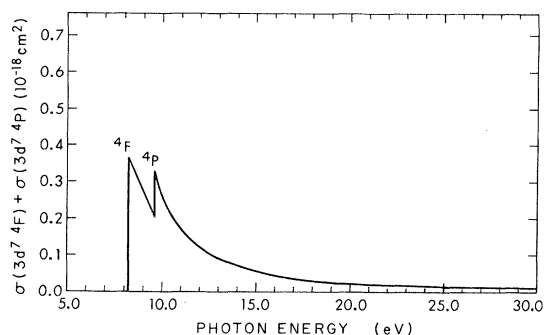


FIG. 2. Cross section for photoionization with excitation for photons incident on the Fe I ground state $(3d)^6 5D(4s)^2 5D$. The resulting Fe II ion is in the excited states $(3d)^7 4F$ or $(3d)^7 4P$.

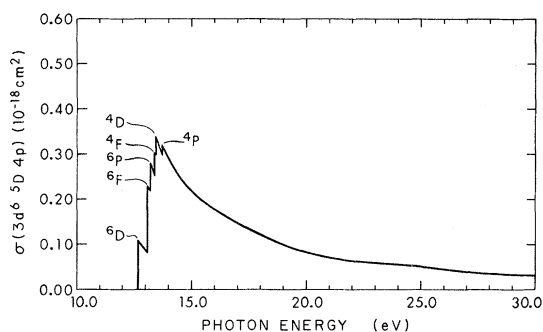


FIG. 3. Cross section for photoionization with excitation for photons incident on Fe I in the ground state with resulting Fe II ion in excited states $(3d)^6 5D(4p) 6D, 6F, 6P, 4F, 4D,$ or $4P$.

given by the diagrams onto the various multiplet states. We also average over values of M_L for our initial state of Fe I. In the calculations we have used the dipole velocity form for the interaction. We note that the dipole length or velocity matrix elements between excited states which occur in the diagrams of Fig. 1(c) can become very large, and especially so if the dipole length formula is used. However, we expect that the results should be insensitive to the use of a cutoff in radial distance in calculating the dipole-matrix elements. We have discussed the use and justification for such cutoffs previously^{20,21} in connection with correlation-energy calculations, and the results in those cases were insensitive to the cutoff. We have found close agreement in this calculation (to within 4%) for cutoffs of $25a_0$ and $10a_0$ where a_0 is the Bohr radius. We have used the results for the $25a_0$ cutoff. In evaluating the diagrams of Fig. 1, we have used our methods for applying many-body perturbation theory to atoms.⁶ The single-particle states have been discussed previously.²² They are essentially Hartree-Fock states for Fe with ex-

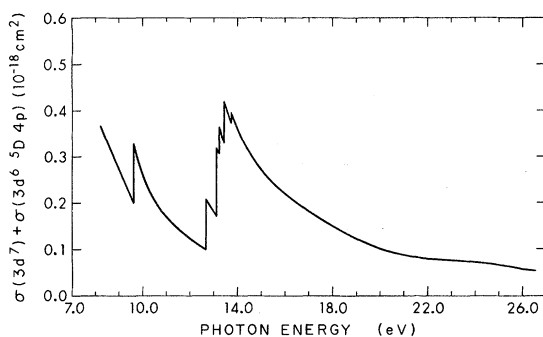


FIG. 4. Sum of photoionization with excitation cross sections of Figs. 2 and 3. The resulting Fe II ion may be in excited states $(3d)^7 4F$ or $4P$, or in states $(3d)^6 5D(4p) 6D, 6F, 6P, 4F, 4D,$ or $4P$.

TABLE I. Cross section for photoionization with excitation for photons incident on Fe I $(3d)^6(4s)^2^5D$.

Photon energy (eV)	$\sigma(^4F) + \sigma(^4P)$ (10^{-18} cm 2) ^a	$\sigma(3d^6 4p)$ (10^{-18} cm 2) ^b	σ excit. (10^{-18} cm 2) ^c
8.1975 ^d	0.366	0.000	0.366
8.500	0.328	0.000	0.328
9.00	0.267	0.000	0.267
9.50	0.208	0.000	0.208
9.586 ^e	(0.199) ^f	0.000	(0.199) ^f
9.800	0.290	0.000	0.290
10.00	0.255	0.000	0.255
10.50	0.206	0.000	0.206
11.00	0.171	0.000	0.171
12.00	0.123	0.000	0.123
12.666 ^g	0.100	0.1094	(0.100) ^f
12.800	0.0960	0.0980	0.194
13.000	0.0912	0.0864	0.178
13.1013 ^h	0.0885	(0.0818) ^f	(0.170) ^f
13.1868 ⁱ	0.0863	(0.2194) ^f	(0.3057) ^f
13.300	0.0840	0.2618	0.3458
13.3821 ^j	0.0815	(0.250) ^f	(0.3314) ^f
13.400	0.0812	0.3023	0.3835
13.4087 ^k	0.0810	(0.3013) ^f	(0.3823) ^f
13.500	0.0790	0.3254	0.4044
13.700	0.0750	0.2995	0.3745
13.7211 ^l	0.0745	(0.2982) ^f	(0.3727) ^f
13.800	0.0730	0.3118	0.3848
14.00	0.0693	0.2920	0.3613
15.00	0.0538	0.2172	0.2710
17.00	0.0336	0.1492	0.1828
20.00	0.0206	0.0808	0.1014
30.00	0.0100	0.0307	0.0407
40.00	0.0096	0.0121	0.0217

^aCross section for Fe II to be left in either of the excited states $3d^7\ ^4F$ or $3d^7\ ^4P$.

^bCross section for Fe II to be left in any one of the excited states $(3d)^6\ ^5D\ 4p\ ^6D$, 6F , 6P , 4F , 4D , or 4P .

^cSum of cross sections in two columns to left.

^dThreshold for $(3d)^7\ ^4F$.

^eThreshold for $(3d)^7\ ^4P$.

^fFigure in parentheses should be associated with number to its right. It is the value for the cross section without the threshold contribution which occurs at that photon energy. When higher-order terms are considered, there will be a series of resonances preceding each threshold in curves of the total cross section.

^gThreshold for $(3d)^6\ ^5D\ 4p\ ^6D$.

^hThreshold for $(3d)^6\ ^5D\ 4p\ ^6F$.

ⁱThreshold for $(3d)^6\ ^5D\ 4p\ ^6P$.

^jThreshold for $(3d)^6\ ^5D\ 4p\ ^4F$.

^kThreshold for $(3d)^6\ ^5D\ 4p\ ^4D$.

^lThreshold for $(3d)^6\ ^5D\ 4p\ ^4P$.

cited states corresponding to physical single-particle excitations.

In Fig. 2 the cross section for excitation of the $(3d)^7\ ^4F$ and $(3d)^7\ ^4P$ states of Fe II is plotted with simultaneous ejection of a 4s electron into the continuum. From angular momentum considerations, the continuum electron can have $l=1$ or $l=3$. Near threshold, $\sigma(\omega)$ is dominated by the $l=1$ continuum contributions. The continuum $l=3$ contributions are negligible near threshold, are approximately equal to the $l=1$ contributions at 25 eV, and then dominate the cross section for higher photon energies.

Also are listed the dominant spectral character-

istics in Tables I and II. In Table I, are given the cross sections for photoionization with excitation. In Table II, the total cross section for photoionization with excitation is listed along with the total cross section for one-electron transitions taken from Ref. 2.

In Fig. 3, we have plotted our results for the cross section $4s^{\pm} \rightarrow 4p$, $4s^{\mp} \rightarrow ks$ or kd , where ks and kd refer to continuum states with $l=0$ and $l=2$, respectively. This leaves Fe II in the configuration $(3d)^6\ ^5D\ 4p$, and the resulting multiplets are 6D , 6F , 6P , 4F , 4D , and 4P . Contributions from the kd states are larger (by approximately 50% on the average) than the ks contributions. Figure 4 shows

TABLE II. Total cross section for photoionization of Fe I $(3d)^6(4s)^2\ ^5D$.

Photon energy (eV)	σ_{excit} (10^{-18} cm 2) ^a	σ (10^{-18} cm 2) ^b	σ_{tot} (10^{-18} cm 2) ^c
7.9004 ^d	0.000	2.210	2.210
8.000	0.000	2.110	2.110
8.1975 ^e	0.366	1.830	2.196
8.446 ^f	0.335	3.055	3.390
9.00	0.267	2.140	2.407
9.50	0.208	1.300	1.508
9.5856 ^g	0.329	1.150	1.479
10.00	0.255	0.515	0.770
10.50	0.206	0.055	0.261
10.789 ^h	0.183	0.535	0.718
11.00	0.171	0.440	0.611
11.50	0.144	0.469	0.613
12.00	0.124	3.55	3.67
12.132 ⁱ	0.118	20.0 ^j	20.12 ^j
12.40	0.109	2.775	2.884
12.6662 ^k	0.209	1.400	1.609
13.00	0.178	0.758	0.936
13.1013 ^l	0.320	0.635	0.955
13.1868 ^m	0.367	0.570	0.937
13.382 ⁿ	0.386	0.450	0.836
13.4087 ^o	0.421	0.438	0.859
13.50	0.404	0.400	0.804
13.7211 ^p	0.396	0.310	0.706
14.00	0.361	0.250	0.611
15.00	0.271	0.391	0.662
15.813 ^q	0.230	3.942	4.172
17.00	0.183	4.411	4.594
20.00	0.101	5.499	5.600
30.00	0.0407	7.742	7.783
40.00	0.0217	8.164	8.186

^aCross section for photoionization which leaves Fe II in one of the excited states $(3d)^7\ ^4F$, 4P , or $(3d)^6\ ^5D(4p)^6D$, 6F , 6P , 4F , 4D , or 4P ; taken from Table I.

^bCross section for one-electron transitions; taken from Ref. 2.

^cSum of σ_{excit} and σ .

^dThreshold for $(3d)^6\ ^5D(4s)^6D$ of Fe II.

^eThreshold for $(3d)^7\ ^4F$.

^fThreshold for $(3d)^6\ ^5D(4s)^4D$.

^gThreshold for $(3d)^7\ ^4P$.

^hThreshold for $(3d)^5\ ^6S(4s)^2\ ^6S$.

ⁱResonance due to degeneracy of $3d \rightarrow 4p$ and $4s \rightarrow kp$ excitation energies. See Ref. 2. Actually, several peaks are expected near this position as discussed in Ref. 2.

^jResonance height not carefully determined. See Ref. 2.

^kThreshold for $(3d)^6\ ^5D(4p)^6D$.

^lThreshold for $(3d)^6\ ^5D(4p)^6F$.

^mThreshold for $(3d)^6\ ^5D(4p)^6P$.

ⁿThreshold for $(3d)^6\ ^5D(4p)^4F$.

^oThreshold for $(3d)^6\ ^5D(4p)^4D$.

^pThreshold for $(3d)^6\ ^5D(4p)^4P$.

^qThreshold for $3d^*$ ionization as discussed in Ref. 2.

Experimentally, one expects to observe separate edges in this vicinity due to $(3d)^5(4s)^2\ ^4P$, 4D , 4F , and 4G .

the combined sum of our contributions to $\sigma(\omega)$ from the low-lying $(3d)^7$ and $(3d)^6\ ^5D(4p)$ excitations of Fe II. Figure 5 gives these results over a larger energy range. We note that there is a resonance

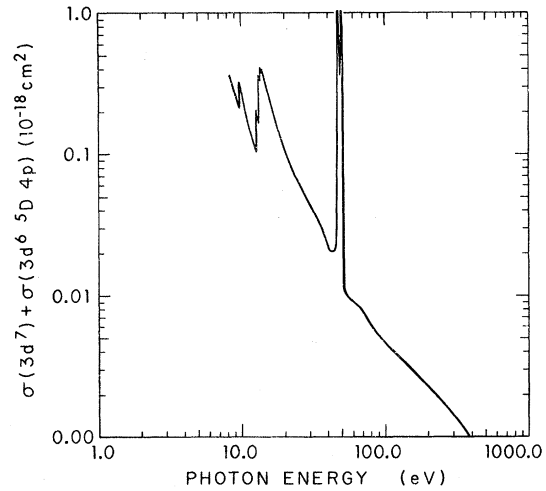


FIG. 5. Sum of photoionization cross sections with excitation in which remaining Fe II ion may be in excited states $(3d)^7\ ^4P$ or 4F or in excited states $(3d)^6\ ^5D(4p)^6D$, 6F , 6P , 4F , 4D , or 4P . The resonances at approximately 49 eV are due to $3p \rightarrow 3d$ excitation which is degenerate in energy with $(4s)^2 \rightarrow 3d kp$.

at approximately 49 eV. This comes from the diagram of Fig. 1(b) with $\beta = 3p$ and $k = 3d$. That is, we have a resonance due to the degeneracy of the $3p \rightarrow 3d$ excitation with $(4s)^2 \rightarrow 3d kp$. The resonance is split according to whether the $(3d)^7$ configuration resulting from $3p \rightarrow 3d$ couples to give the 4P or 4F multiplet. There should be splitting due to $3p_{3/2}$ and $3p_{1/2}$ splitting, but we have not taken this into account.

In Fig. 6, the single-electron photoionization cross section taken from our previous Fe calculation² is plotted in a solid line. The dashed line is our new value for the total cross section. It con-

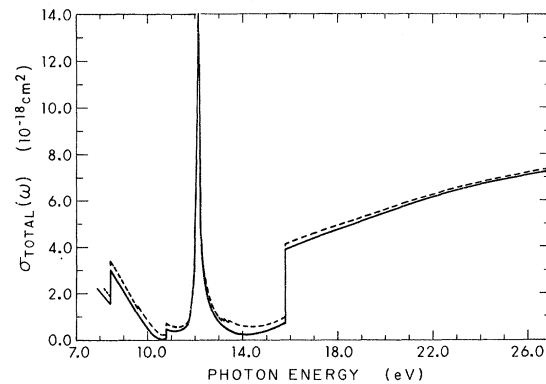


FIG. 6. Total photoionization cross section for Fe I. The solid curve is the cross section without excitation and is taken from Ref. 2. The dashed curve includes excitation to the $(3d)^7$ and $(3d)^6\ ^5D(4p)$ configurations of Fe II as given in Figs. 4 or 5.

sists of the results of Fig. 4 plus the solid curve. At threshold for the $(3d)^7 4F$ excitation, the ratio of the results of Fig. 4 to the photoionization without excitation (given by the solid curve of Fig. 6) is approximately 0.20. The ratio varies greatly with variations in $\sigma(\omega)$ given by the solid curve of Fig. 6. On the average, however, the dashed cross section of Fig. 6 is at least 20% greater than the cross section given by the solid curve in the range 8.2–16.0 eV. Since we have not yet calculated the higher-order diagrams contributing to the $(3d)^7$ and $(3d)^6 5D(4p)$ excitations of Fe II our calculated results are probably uncertain to at least 25%.

There may also be significant contributions to the total cross section from excitations to other states of Fe II which we have not yet considered, such as the $(3d)^6 5D(ns)$ states with $n \geq 5$. There are also contributions to the total cross section in which two or more electrons are ejected into continuum states (double or higher photoionization). For neon, Wuilleumier and Krause^{8,12} found that

multiple processes (excitation and double photoionization) are approximately 20% of the total photo-cross-section at all energies except near ionization thresholds. They attribute approximately $\frac{1}{3}$ of the multiple processes to excitation of bound states and the remaining $\frac{2}{3}$ to double photoionization. They also found that for neon the most important processes of photoionization with excitation are those in which the ejected electron goes to a continuum state with $l' = l \pm 1$ while the excited electron goes to a state with $l' = l$. This would suggest that for Fe there may be appreciable contributions from excitations into $(3d)^6 5D(ns)$ states. It is clear that accurate calculations of photoionization cross sections must include effects from multiple processes. We intend to continue these investigations for other excited states of Fe II and also for other atoms.

ACKNOWLEDGMENT

I wish to thank Dr. Manfred O. Krause for helpful discussions.

†Research supported by the Aerospace Research Laboratories, Office of Aerospace Research, U. S. Air Force, contract No. F33615-69-C-1048.

¹G. V. Marr, *Photoionization Processes in Gases* (Academic, New York, 1967).

²H. P. Kelly and A. Ron, *Phys. Rev. A* **5**, 168 (1972).

³O. Gingerich (private communication).

⁴K. A. Brueckner, *Phys. Rev.* **97**, 1353 (1955); *The Many-Body Problem* (Wiley, New York, 1959).

⁵J. Goldstone, *Proc. Roy. Soc. (London)* **A239**, 267 (1957).

⁶H. P. Kelly, *Phys. Rev.* **136**, B896 (1964).

⁷J. A. R. Samson, *Phys. Rev. Letters* **22**, 693 (1969).

⁸F. Wuilleumier and M. O. Krause, *J. Phys. B* (to be published); T. A. Carlson, M. O. Krause, and W. E. Moddeman, *J. Phys. (Paris)* **32**, C4-76 (1971).

⁹E. E. Salpeter and M. H. Zaidi, *Phys. Rev.* **125**, 248 (1962).

¹⁰R. Brown, *Phys. Rev. A* **1**, 341 (1970).

¹¹V. Jacobs, *Phys. Rev. A* **3**, 289 (1971).

¹²F. Wuilleumier and M. O. Krause, in *Proceedings of the International Conference on Electron Spectroscopy,*

Asilomar, California, 1971 (North-Holland, Amsterdam, 1972).

¹³A. Dalgarno, in *Perturbation Theory and Its Applications in Quantum Mechanics*, edited by C. H. Wilcox (Wiley, New York, 1966), p. 145.

¹⁴H. P. Kelly, *Correlation Structure in Atoms* (Academic, New York, 1968), Vol. 2, p. 75.

¹⁵H. P. Kelly, *Phys. Rev.* **182**, 84 (1969).

¹⁶H. A. Bethe and E. E. Salpeter, *Quantum Mechanics of One- and Two-Electron Atoms* (Academic, New York, 1957), p. 252.

¹⁷M. Ya. Amusia and M. P. Kazachkov, *Phys. Letters* **28A**, 27 (1968).

¹⁸T. N. Chang, T. Ishihara, and R. T. Poe, *Phys. Rev. Letters* **27**, 838 (1971).

¹⁹C. E. Moore, *Atomic Energy Levels*, Natl. Bur. Std. Circ. No. 467 (U. S. GPO, Washington, D. C., 1949).

²⁰H. P. Kelly, *Phys. Rev.* **131**, 684 (1963).

²¹H. P. Kelly, *Phys. Rev.* **144**, 39 (1966).

²²H. Kelly and A. Ron, *Phys. Rev. A* **2**, 1261 (1970).